The stress–life fatigue behaviour of aluminium alloy foams

K. Y. G. McCULLOUGH, N. A. FLECK and M. F. ASHBY

Engineering Department, Cambridge University, Trumpington Street, Cambridge CB2 1PZ, UK

Received in final form 28 October 1999

ABSTRACT The tension–tension and compression–compression nominal stress versus fatigue life responses of Alulight closed cell aluminium alloy foams have been measured for the compositions Al–1Mg–0.6Si and Al–1Mg–10Si (wt%), and for relative densities in the range 0.1–0.4. The fatigue strength of each foam increases with the relative density and with the mean applied stress, and is greater for the transverse orientation than for the longitudinal orientation. Under both tension–tension and compression–compression loading the dominant cyclic deformation mode appears to be material ratchetting; consequently, the fatigue life is highly sensitive to the magnitude of the applied stress. A micromechanical model is given to predict the dependence of life upon stress level and relative density. Panels containing a central hole were found to be notch insensitive for both tension–tension and compression–compression fatigue loading: the net-section strength equals the unnotched strength.

Keywords metallic foam, aluminium alloys, stress–life curves, fatigue life, ratchetting.

NOMENCLATURE

B = specimen thickness
C, n, p, q, σ_0 = material parameters used in the ratchetting model
D = hole diameter for panels containing a central through-hole
E = unloading modulus
F = applied load
K_T = elastic stress concentration factor
l = cell size
L = specimen length
N, N_f = number of fatigue cycles and fatigue life, respectively
R = load ratio defined by $R \equiv |\sigma|_{min}/|\sigma|_{max}$
t = cell edge thickness
W = specimen width
β = angle between the normal to the crush front and the axial direction
$\dot{\delta}$ = deflection rate of the cell edge
$\varepsilon, \dot{\varepsilon}$ = nominal axial strain and strain rate, respectively
ε_y = monotonic yield strain
γ = shear component of strain in the crush band
$\bar{\rho}$ = relative density = foam density/density of the cell edge material
σ_y = monotonic yield strength (which is equal in tension and compression)
$|\sigma|_{max}, |\sigma|_{min}$ = magnitudes of the maximum and minimum nominal applied stresses
$|\sigma|_{max,n}, |\sigma|_{max,un}$ = fatigue limits of notched and un-notched specimen, respectively

INTRODUCTION

Recently, a range of aluminium alloy foams have become commercially available, due to developments in processing methods and to a market need for ultra-lightweight structures (see Ref. [1] for a review of current understanding). As metallic foams become cheaper, more uniform in microstructure and more reproducible in properties, they are increasingly attractive for use in monolithic form or as the cores of sandwich panels. It is anticipated that the fatigue strength of metallic foams

Correspondence: N. A. Fleck. Fax +44 1223 332662.
E-mail: naf1@eng.cam.ac.uk

is of primary concern in practical applications, necessitating the generation of fatigue design data.

This paper reports a detailed study of the fatigue response of one range of aluminium alloy foams marketed under the trade-name 'Alulight'. Alulight is a closed-cell foam produced by a powder route,[2] and is available as plates or cylinders with a relative density $\bar{\rho}$ ranging from 0.1 to 0.4, and with compositions Al–1Mg–0.6Si and Al–1Mg–10Si (wt %). An optical cross-sectional view of the resultant structure is shown in Fig. 1(a), and typical tensile and compressive nominal stress–strain curves are given in Fig. 1(b) and (c), respectively.

In order to compare the fatigue strength with the monotonic strength, the applied loading, characterized by $|\sigma|_{max}$, will be normalized by the monotonic yield strength σ_y of the specimen. Under compressive loading this yield strength is defined at an offset plastic strain of 2%, whilst under tensile loading it is taken as the peak stress sustained by the specimen.[3] The tensile and compressive yield strengths of the Alulight foams are approximately equal but are sensitive to the relative density, $\bar{\rho}$, defined by the density of the foam divided by that of the cell edge material. For values of $\bar{\rho}$ in the range 0.1–0.4, the yield strengths of the Al–1Mg–0.6Si and Al–1Mg–10Si can be adequately described by the following simple power law fits[3]

Al–1Mg–0.6Si:

Longitudinal orientation	Transverse orientation
$\sigma_y = 94\bar{\rho}^{1.5}$ (MPa)	$\sigma_y = 70\bar{\rho}^{1.5}$ (MPa)

Al–1Mg–10Si:

Longitudinal orientation	Transverse orientation
$\sigma_y = 64\bar{\rho}^{1.5}$ (MPa)	$\sigma_y = 48\bar{\rho}^{1.5}$ (MPa)

(1)

MATERIAL SPECIFICATION AND EXPERIMENTAL PROCEDURE

Alulight foam sandwich panels of dimension 145 × 145 × 9 mm were obtained with two compositions, Al–1Mg–0.6Si and Al–1Mg–10Si (wt%). The panels have solid skins of thickness 0.75 mm and a foam core. Because the primary focus of this study is the effect of foam density and composition upon the stress–life fatigue response, the skins were removed by wire electro-discharge machining, giving a net specimen thickness B of 7.5 mm (5–15 cells, depending upon the relative density). Test specimens with relative densities in the range $\bar{\rho} = 0.1$–0.4 were electro-discharge machined from the foam plates; the precise value of $\bar{\rho}$ for each specimen

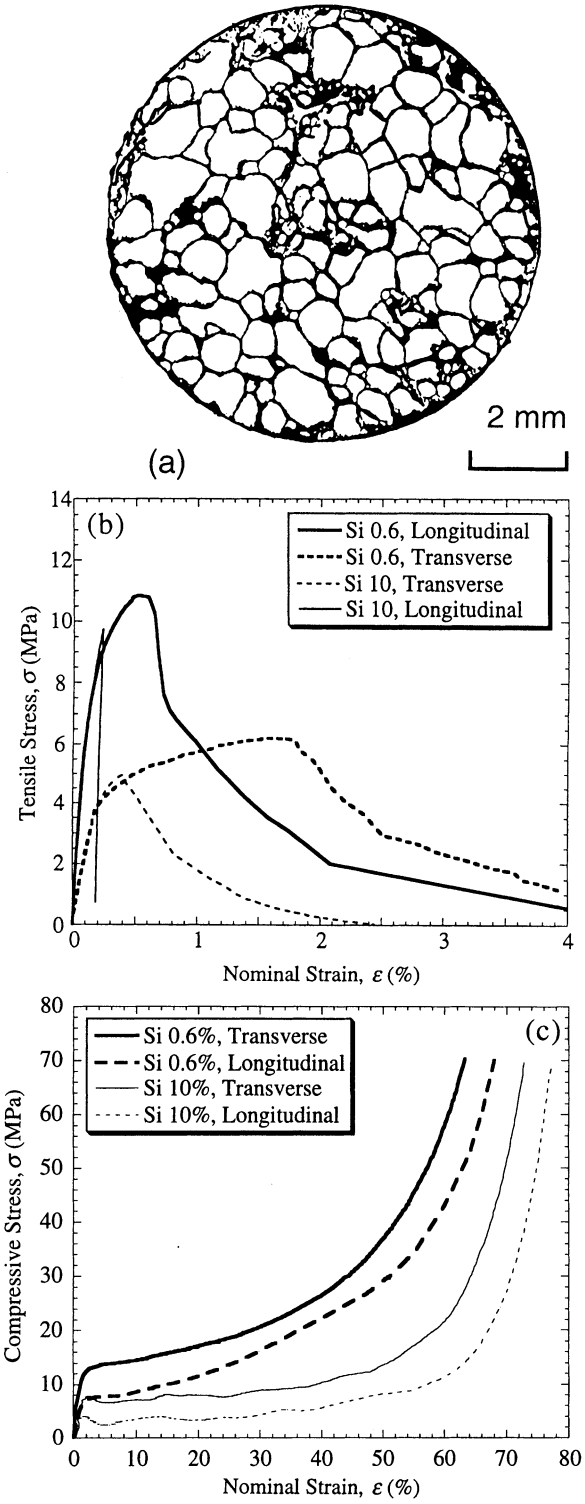

Fig. 1 The Alulight aluminium alloy foam. (a) Optical cross-sectional view (reproduced from Sugimura *et al.*[6]). (b) Typical tensile stress–strain responses for foams with $\bar{\rho} = 0.25$. (c) Typical compressive stress–strain responses for foams with $\bar{\rho} = 0.25$ (reproduced from McCullough *et al.*[3]).

was obtained by accurate weighing (to four significant figures). Dogbone-type specimens (of overall dimension 70 × 20 × 7.5 mm with a gauge section 10 × 10 × 7.5 mm and a neck radius of 25 mm) and cuboid-shaped specimens (15 × 10 × 7.5 mm) were used for the tension–tension and compression–compression tests, respectively. Specimens with these dimensions have been found to be sufficiently large to avoid free-surface effects.[3,4]

Geometric constraints in the manufacturing process of Alulight are known to lead to the formation of ellipsoidal-shaped cells.[2,3] Consequently, the unloading modulus E and the yield strength σ_y of foams loaded in the transverse orientation of the foamed plates are 25% less than the corresponding values in the longitudinal orientation.[3] Specimens were cut and loaded in both directions.

Fatigue tests were performed at room temperature, using constant values of maximum and minimum load and a frequency of 50 Hz. (Preliminary tests confirmed that the fatigue stress–life behaviour was independent of the loading frequency over the range 1–70 Hz.) The compression–compression fatigue tests were performed using flat loading platens lubricated with PTFE spray, and the nominal strain was calculated from the grip displacement. In the tension tests, a clip gauge of gauge length 10 mm was used to measure the nominal axial strain. The peak values of load and nominal strain were recorded continuously throughout each test. The load ratio R was defined as the ratio of the minimum to the maximum values of the absolute nominal stress

$$R \equiv \frac{|\sigma|_{\min}}{|\sigma|_{\max}} \tag{2}$$

STRESS–LIFE RESPONSES UNDER $R = 0.1$ FATIGUE LOADING

In this section, the tension–tension and compression–compression fatigue responses are reported for Al–1Mg–0.6Si foam, with a relative density $\bar{\rho} = 0.29$–0.35. The specimens were loaded in the longitudinal orientation, with a load ratio $R = 0.1$. Hereafter, we shall refer to such foams as 'high-density' foams, to differentiate them from 'low-density' foams of relative density $\bar{\rho} =$ 0.15–0.18.

Tension–tension fatigue response

Under tension–tension cyclic loading, specimens progressively lengthened with increasing fatigue cycles until material separation occurred at an accumulated axial strain of ~1%. Typical responses are shown in Fig. 2(a),

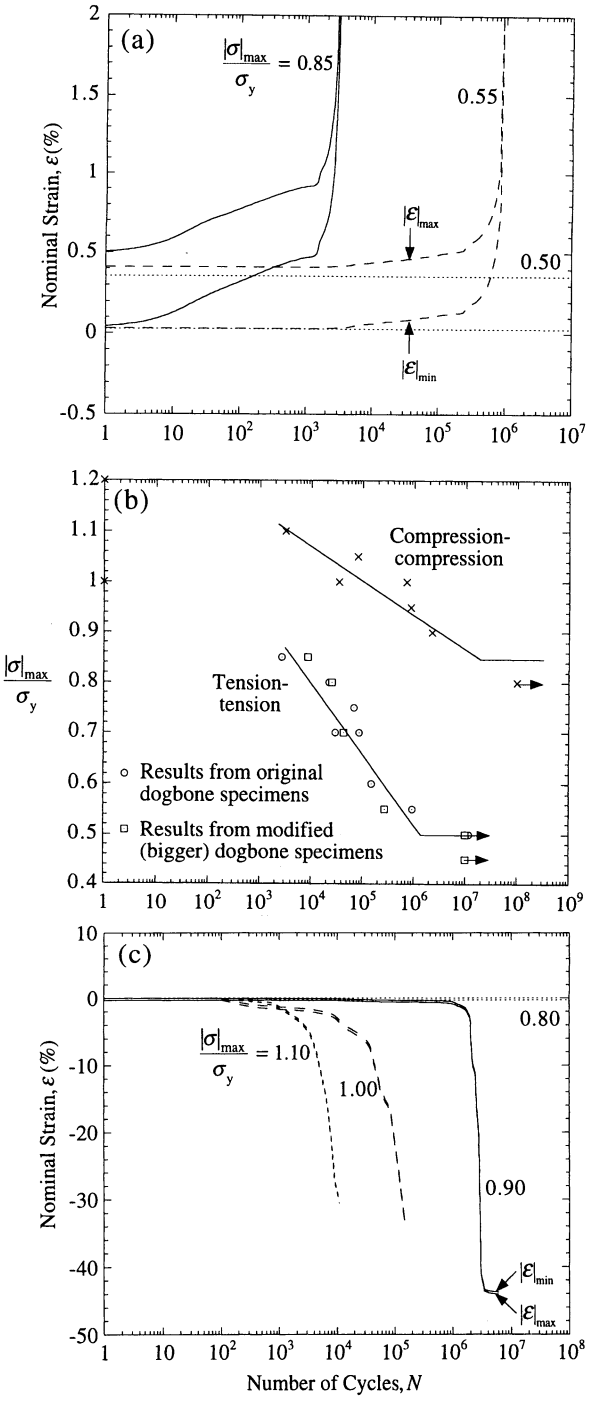

Fig. 2 Typical responses of Al–1Mg–0.6Si under $R = 0.1$ fatigue loading; specimens with $\bar{\rho} = 0.29$–0.35 which were tested in the longitudinal orientation. (a) Accumulation of maximum and minimum strain with cycles for specimens under tension–tension loading. (b) Comparison of tension–tension and compression–compression S–N curves. (c) Accumulation of maximum and minimum strain with cycles for specimens under compression–compression loading.

wherein the nominal axial strains $|\varepsilon|_{max}$ and $|\varepsilon|_{min}$ at the peak loads of the fatigue cycle are plotted against the number of fatigue cycles N. The fatigue life N_f is defined as the number of fatigue cycles to material separation, at any given stress level $|\sigma|_{max}/\sigma_y$. The failure strain of $|\varepsilon|_{max} \sim 1\%$ is approximately equal to that recorded in corresponding monotonic tests,[3] and is relatively insensitive to the applied stress level. It is instructive to construct a stress–life (S–N) curve by plotting the fatigue life against $|\sigma|_{max}/\sigma_y$, as shown in Fig. 2(b). It is noted from the figure that the fatigue limit, defined by the ratio $|\sigma|_{max}/\sigma_y$ at a fatigue life of 10^7 cycles, equals 0.5 for the high-density Al–1Mg–0.6Si foam.

Compression–compression fatigue response

Under compression–compression fatigue loading with $|\sigma|_{max}/\sigma_y \sim 0.8$, progressive shortening is observed, as shown in Fig. 2(c). The accumulated strains $|\varepsilon|_{max}$ and $|\varepsilon|_{min}$ are plotted against the number of fatigue cycles N, for tests performed at selected levels of $|\sigma|_{max}/\sigma_y$. In contrast to the low levels of accumulated strain in tension–tension fatigue, large plastic strains of the order of 50% develop in compression–compression fatigue. The range of strain within each fatigue cycle is much less than the compressive plastic strain accumulated during the whole test. In practical applications, such shortening would not usually be acceptable and would be treated as 'failure' of the component.

It is clear from each of the curves of Fig. 2(c) that an initial incubation period exists during which the specimen progressively shortens at a slow rate. A knee in the curve occurs at $|\varepsilon|_{max} \sim 2\%$, beyond which the specimen shortens at an increased rate (typically 20–30 times faster). During this phase of rapid shortening, a crush band propagates along the length of the specimen. At a nominal strain of $\sim$40%, the crush band has propagated throughout the specimen, and opposing cell faces touch. The rate of accumulated plastic strain per cycle then decreases sharply. We shall define the fatigue life of the foam N_f as the number of cycles at the knee of the $|\varepsilon|_{max}$ versus N_f curve; this definition agrees with that of Sugimura *et al.*[5] in a companion study on Alporas metallic foam.

The S–N curve for compression–compression loading is plotted in Fig. 2(b). We note that the fatigue life equals 10^7 cycles at $|\sigma|_{max}/\sigma_y \sim 0.85$, and we shall take this value as the fatigue limit in compression for $R = 0.1$. As in the tensile fatigue tests, specimens tested at stress levels less than or equal to the fatigue limit sustain negligible permanent deformation, and an optical microscope examination revealed no cell edge cracking or buckling. To confirm this, five specimens were tested in compression–compression loading at stress levels below the fatigue limit for 10^7 cycles; none of the specimens failed, and they were then reloaded at stress levels above the fatigue limit. The subsequent fatigue lives were indistinguishable (within material scatter) from the results of previously untested specimens.

Comparison of the tension–tension and compression–compression results

The scatter of the results shown in Fig. 2(b) reflects the stochastic nature of the deformation of Alulight under both tension–tension and compression–compression loadings; nominally identical tests give fatigue lives which may differ by over a decade. Such material scatter is common to all tests performed on commercially available closed-cell aluminium alloy foams; there is mounting evidence that this scatter is caused by imperfections in the cellular microstructure. The most significant imperfections are thought to be inhomogeneity (and, in particular, redundant solid material or large isolated voids) and the presence of morphological defects, e.g. cells with large Plateau borders (material concentrated at cell nodes rather than at cell edges), cells with wiggly, buckled or broken edges, or cells with damaged cell faces.[1,3,6–8]

From Fig. 2(b), the fatigue limit of $|\sigma|_{max}/\sigma_y \sim 0.5$ for tension–tension loading is $\sim$40% less than the value of $|\sigma|_{max}/\sigma_y \sim 0.85$ for compression–compression loading. A similar difference was observed in tests performed on specimens loaded in the transverse orientation. To ensure that this was not an artefact of the geometry of the tensile specimens, further tension–tension tests were performed on modified dogbone specimens: the specimen width was increased by a factor of four, the total length was doubled, and the fully dense reinforcing skins were not removed from the gripped portions of the dogbones in order to encourage failure within the gauge section. The results from these modified specimens were indistinguishable (within the limits of material scatter) from those outlined above, see Fig. 2(b).

EFFECT OF RELATIVE DENSITY, SILICON CONTENT AND MEAN STRESS ON THE COMPRESSION–COMPRESSION FATIGUE RESPONSE

Compression–compression tests at $R = 0.1$ were performed on longitudinally cut Al–1Mg–0.6Si specimens made from low-density foam ($\bar{\rho} = 0.15$–0.18) and high-density foam ($\bar{\rho} = 0.34$–0.36). The responses of accumulated strain versus cycles were qualitatively similar for the low- and high-density specimens, and are not reproduced here. For both low- and high-density foam, the strain level at the knee of the strain–cycles curve is comparable with the monotonic yield strain ($|\varepsilon|_{max} \sim 1\%$

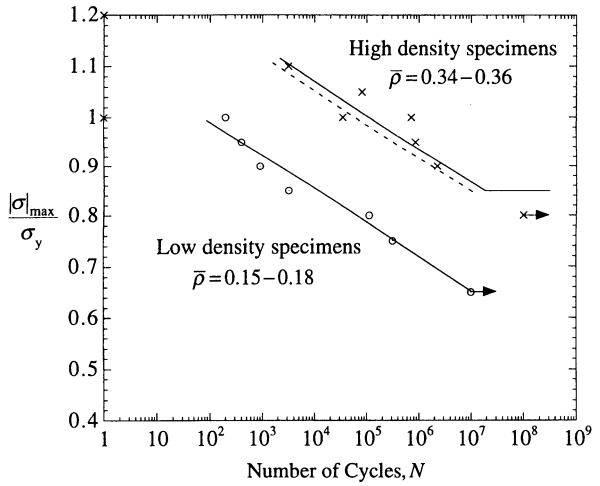

Fig. 3 Effect of relative density on the stress–life curve of Al–1Mg–0.6Si, for compression–compression fatigue at $R = 0.1$ on specimens tested in the longitudinal orientation. The solid lines give the *S–N* curves for fatigue life defined by the knee of the accumulated strain versus cycles curve. The dashed lines show the *S–N* curves where the fatigue life has been defined at $|\varepsilon|_{max} = 1\%$. For the low-density specimens the dashed and solid lines coincide.

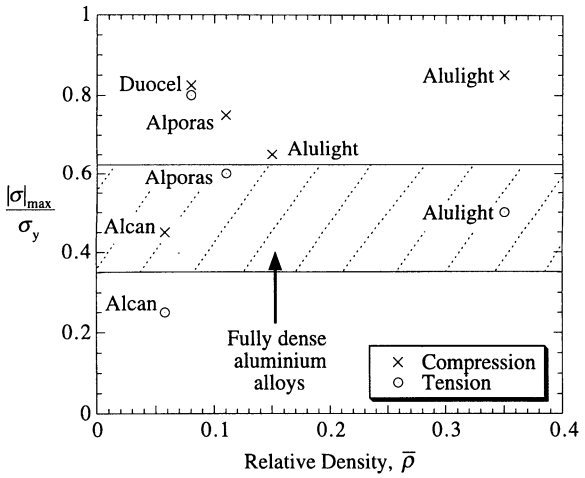

Fig. 4 Comparison of the fatigue limits of aluminium alloy foams at $R = 0.1$. The Alulight data are shown for Al–1Mg–0.6Si where the specimens were tested in the longitudinal orientation.

for low-density foams, $|\varepsilon|_{max} \sim 2\%$ for high). The resulting *S–N* curves are compared in Fig. 3. The fatigue limit of the low-density specimens is $|\sigma|_{max}/\sigma_y \sim 0.65$, which is ~20% less than the fatigue limit of the high-density specimens, $|\sigma|_{max}/\sigma_y \sim 0.85$. So far, the fatigue life has been defined by the knee in the $|\varepsilon|_{max}$ versus N curve. If instead, the fatigue life is defined at a prescribed strain level of $|\varepsilon|_{max} \sim 1\%$, the *S–N* curves remain virtually unchanged.

The fatigue limits of Alulight Al–1Mg–0.6Si, tested in the longitudinal orientation under a fixed load ratio $R = 0.1$, are plotted against relative density $\bar{\rho}$ in Fig. 4. For comparison, the fatigue limits of the ERG Duocel open cell,[9] and the Alporas[9] and Alcan[10] closed-cell foams have been included. Also shown are the fatigue limits for tension–tension fatigue of fully dense aluminium alloys, where σ_y denotes the 0.2% offset tensile yield strength. The fatigue ratio of the foams is of similar magnitude to that observed for fully dense aluminium alloys.

In order to investigate the compression–compression shortening response, video recordings were taken of each test. Figure 5(a) shows typical micrographs from a test performed on a low-density ($\bar{\rho} = 0.15$) cuboid specimen, loaded in the longitudinal orientation of the foamed plates at an applied stress $|\sigma|_{max}/\sigma_y = 1.05$, with $R = 0.1$. Figure 5(b) shows typical micrographs from a test on a high density ($\bar{\rho} = 0.35$) specimen, again with $|\sigma|_{max}/\sigma_y = 1.05$ and $R = 0.1$. For both densities the progressive buckling of cell edges is evident.

A comparison of Fig. 5(a) and (b) reveals some qualitative differences. For the low-density specimens the crush band develops transversely and then propagates axially. In contrast, for the high-density specimens the crush front is inclined at an angle $\beta \sim 25°$ to the transverse direction. The transition from a crush band inclination of $\beta \sim 0°$ to $\beta \sim 25°$ occurs at a relative density ~0.25. The nominal compressive strain ε within the band in the low-density specimens is ~40%. In the high-density specimens, the inclined crush band broadens with a constant strain, comprising a direct compressive strain ε of ~40% along the normal to the band, and a shear strain γ of ~40% in axes aligned with the boundary of the band.

Effect of silicon content and specimen orientation on the compression–compression *S–N* curve

Under monotonic tensile loading, the Al–1Mg–10Si foam has lower values of fracture toughness, yield strength, unloading modulus and ductility than the Al–1Mg–0.6Si foam.[3,11] Our tests show that its fatigue strength, also, is lower and that the knee in the $|\varepsilon|$ versus N curve occurs at a strain level of $|\varepsilon|_{max} \sim 0.5\%$; this is approximately a quarter of the value $|\varepsilon|_{max} \sim 2\%$ observed for the 0.6% Si foam of comparable relative density. For both compositions, the strain level at the knee of the strain versus cycles curve is comparable with the monotonic yield strain. We continue to use this knee as the definition of fatigue failure. The resulting *S–N* curves for the 10% Si and 0.6% Si foams are compared in Fig. 6(a) by plotting $|\sigma|_{max}/\sigma_y$ versus N_f, revealing that the fatigue strength normalized by the monotonic strength is less for the 10% Si foam than for the 0.6% Si foam. Upon comparing this result with that observed in Fig. 3 for the low-density 0.6% Si foam, a correlation

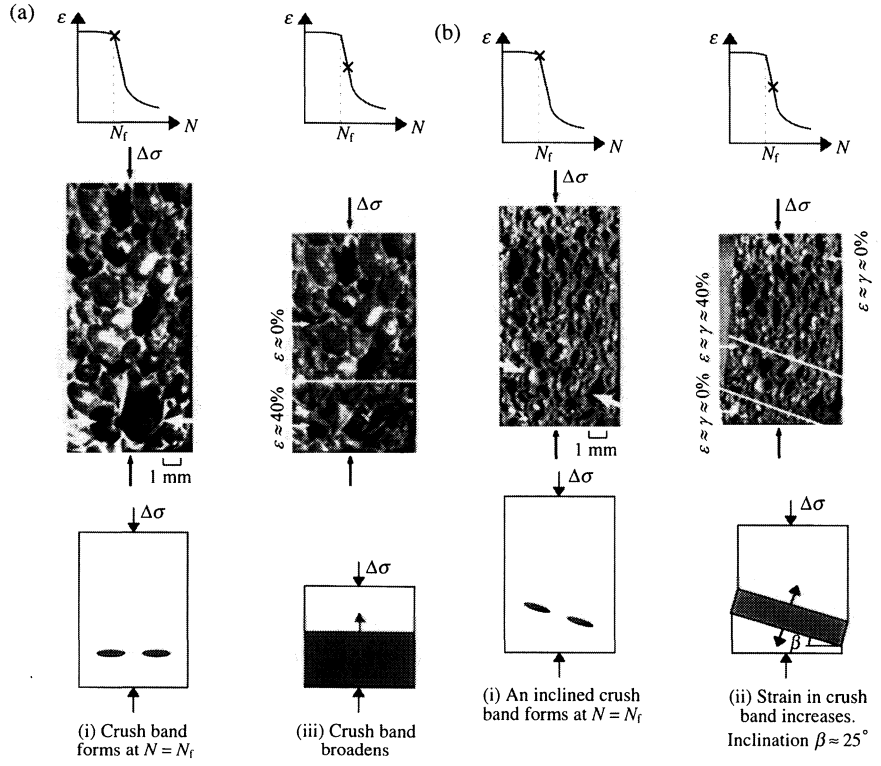

Fig. 5 Progressive shortening response of Al–1Mg–0.6Si specimens under compression–compression loading in the longitudinal orientation, with $|\sigma|_{max}/\sigma_y = 1.05$ and $R = 0.1$. (a) For low-density ($\bar{\rho} = 0.15$) foam and (b) for high-density ($\bar{\rho} = 0.35$) foam.

emerges between the normalized fatigue limit and the monotonic compressive yield strain of the foam: the lower the yield strain, the smaller the normalized fatigue limit.

The *S–N* curves for transversely loaded Al–1Mg–0.6Si specimens, of relative density $\bar{\rho} = 0.31$–0.36, are included in Fig. 6(a): the fatigue ratio at 10^7 cycles equals 0.95, which is slightly greater than the value of 0.85 in the longitudinal direction.

Effect of mean stress on the compression–compression response

Compression–compression tests were performed on the Al–1Mg–0.6Si foam at a fixed load ratio $R = 0.5$, in addition to the $R = 0.1$ tests. Typical plots of the accumulated maximum and minimum strain with cycles are shown in Fig. 6(b), here using a linear rather than a log scale. The compression–compression response at $R = 0.5$ is markedly different from that at $R = 0.1$ [Fig. 2(c)]. At $R = 0.5$, the accumulated macroscopic strain is due to the sequential crushing of spatially random rows of cells, rather than due to the formation and broadening of a single crush band. The steps in the strain versus cycles curve at $|\sigma|_{max}/\sigma_y = 1.5$ are due to the sequential formation of randomly located crush bands, a response also reported for Alcan aluminium foams.[10] Significant cyclic hardening occurs at $R = 0.5$, resulting in a fatigue limit 30% greater than the monotonic yield strength, see Fig. 6(b).

FATIGUE MECHANISMS

The fatigue life has been defined herein by the knee of the accumulated strain versus cycles curve, with the knee occurring at a strain level of 0.5–2%, which is comparable to the monotonic yield strain. It is now argued that the fatigue life under compression–compression loading and tension–tension loading is controlled by the progressive accumulation of strain by material ratchetting, and not by cracking events within the foam. It is envisaged that deformation accumulates within the weakest cross-section of the foam, by ratchetting of the cell edges (Fig. 7); this deformation mode is analogous to creep buckling in compression and creep extension in tension. The evidence is as follows.

1 The tension–tension and compression–compression *S–N* curves shown in Fig. 2(b) are adequately described by power law fits with slopes of $\sim -1/20$. The very high sensitivity of fatigue life to the magnitude of the applied stress suggests that ratchetting (cyclic creep) is the dominant deformation process under tension–tension and compression–compression loading (see, e.g. Ref. [12]).

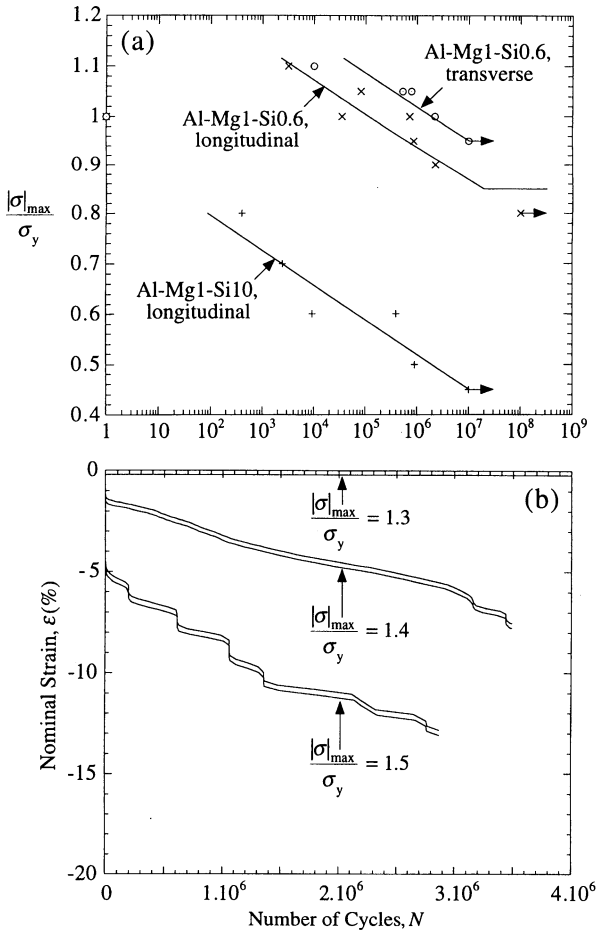

Fig. 6 Further compression–compression results. (a) Effect of silicon content and specimen orientation on the compression–compression S–N curve at $R = 0.1$. Results shown for specimens with $\bar{\rho} = 0.30$–0.36. (b) Effect of mean stress on the compression–compression fatigue response. Accumulation of strain with cycles for Al–1Mg–0.6Si in compression–compression fatigue at $R = 0.5$; specimens with $\bar{\rho} = 0.34$–0.36 which were tested in the longitudinal orientation.

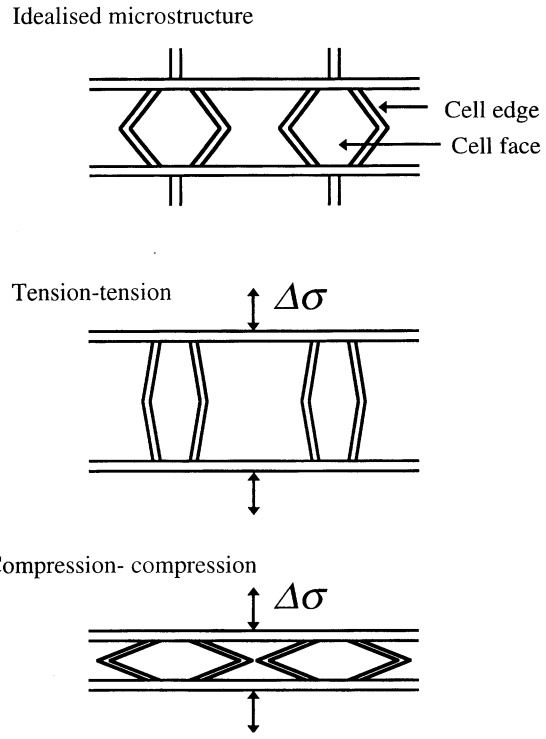

Fig. 7 Deformation mechanisms of an idealized microstructure.

2 Under both tension–tension and compression–compression loading, the foam ratchets almost immediately, provided the applied stress level exceeds the fatigue limit, see Fig. 2(a) and (c).
3 *In situ* optical microscopy and video recordings were used to examine the progression of deformation and cracking within the foam, for both tension–tension and compression–compression fatigue. No cell edge cracking (and minimal cell face cracking) was observed prior to the attainment of the fatigue life, for both directions of loading. This suggests that material ratchetting dominates the fatigue life, and not tensile cracking.
4 In tension–tension fatigue, the propagation of a single, dominant tensile crack across the specimen section occurs after the knee of the strain versus cycles curve. Alternatively, in compression–compression fatigue, the propagation of crush bands along the loading direction also occurs after the knee of the strain versus cycles curve.
5 Examination of the fracture surfaces of the fatigue specimens after tension–tension loading was performed using a scanning electron microscope (SEM). A typical micrograph is given in Fig. 8(a), and a micrograph of the failure surface after a monotonic tension test is given in Fig. 8(b) for comparison. The micromechanism of failure is the same for both monotonic and cyclic loading: microvoid coalescence is evident.

We conclude that the rate-determining step for fatigue failure is the formation of the crush band in compression–compression fatigue, and by rupture of the cross-section in tension–tension fatigue.

A micromechanical model to predict the fatigue life

A simple model for predicting the fatigue life of the foam under tension–tension or compression–compression loading is developed by modifying the creep model of Gibson and Ashby,[13] as follows. Gibson and Ashby consider the case of a foam for which the cell edges undergo power law creep in uniaxial tension

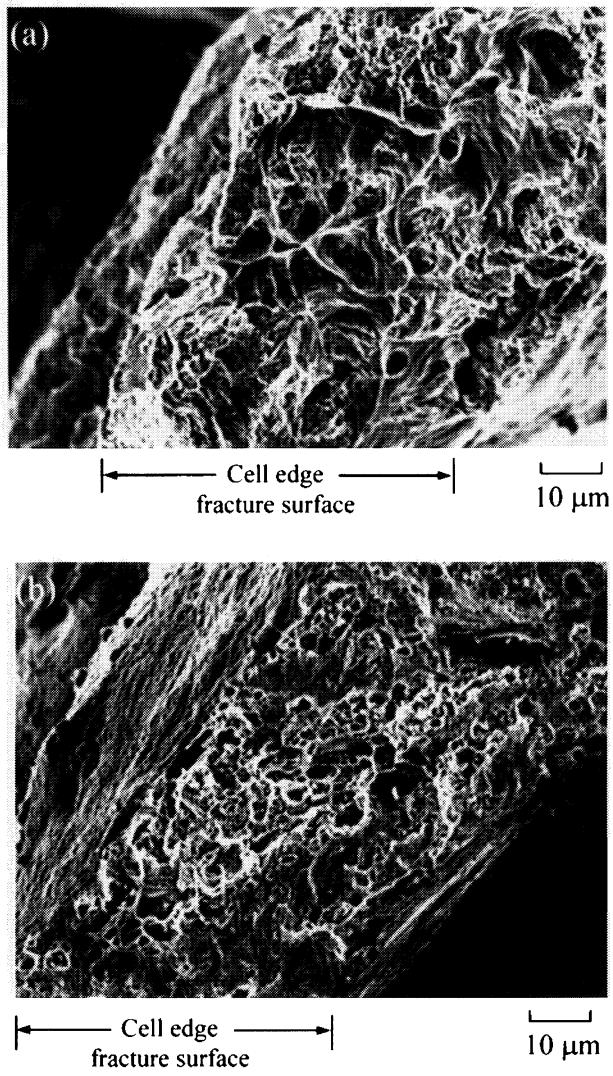

Fig. 8 Comparison of SEM micrographs of the fracture surfaces from cyclic and monotonic tension tests on Al–1Mg–0.6Si. (a) Tension–tension fatigue test at $R = 0.1$ on a specimen with $\bar{\rho} = 0.26$. (b) Monotonic tension test on a specimen with $\bar{\rho} = 0.33$.

according to

$$\dot{\varepsilon} = C\left(\frac{\sigma}{\sigma_0}\right)^n \tag{3}$$

where C, σ_0 and the exponent n are creep constants. In analogous fashion, we follow the suggestion of Megahed *et al.*,[12] and assume that the rate of material ratchetting $d\varepsilon/dN$ of the cell edge material in uniaxial cyclic tension is given by the relation

$$\frac{d\varepsilon}{dN} = C\left(\frac{\Delta\sigma}{\sigma_0}\right)^p\left(\frac{\sigma_{max}}{\sigma_0}\right)^q \tag{4}$$

where C, σ_0, p and q are material constants. Typically, for face-centred cubic metals we find $p \sim q/5$ and q is in the range 4–20, with $q \sim 13$ for aluminium.[12,14,15] We note that Eq. (4) can be brought into close agreement with Eq. (3) if we replace the role of cycles N by time, and if we write $\Delta\sigma = (1-R)|\sigma|_{max}$, giving

$$\frac{d\varepsilon}{dN} = C(1-R)^p\left(\frac{\sigma_{max}}{\sigma_0}\right)^n \tag{5}$$

where $n = p + q$.

The accumulation of plastic strain up to the fatigue life of the foam may be estimated by assuming the underlying cell edge material undergoes ratchetting, just as in the creep case the creep life is dictated by creep deformation of the cell edges. First consider the creep of cell edges within a foam loaded by a cell edge force F as shown in Fig. 9. The deflection rate of the cell edge $\dot{\delta}$ is found to be [Eq. (6.7) from Gibson and Ashby[13]]

$$\dot{\delta} = \frac{C}{4(n+2)}\frac{l^2}{t}\left[\left(\frac{2n+1}{4n}\right)\frac{Fl}{\sigma_0 t^3}\right]^n \tag{6}$$

in terms of the applied load F, the cell size $2l$ and the cell edge thickness t. Now, the load F is proportional to σl^2, where σ is the macroscopic stress on the foam; the overall strain rate $\dot{\varepsilon}$ of the foam is proportional to $\dot{\delta}/l$. For open cell foams, this gives

$$\dot{\varepsilon} = C\frac{C_9}{n+2}\left[\frac{C_{10}(2n+1)}{n}\frac{\sigma}{\sigma_0}\right]^n \bar{\rho}^{(3n+1)/2} \tag{7}$$

where C_9 and C_{10} are constants, following the notation of Gibson and Ashby.[13] The correct behaviours in the limit of linear behaviour $n = 1$ and in the rigid-ideally plastic limit, $n = \infty$ are recovered by taking $C_9 = 0.6$ and $C_{10} = 1.7$. To proceed, we translate the result[7] directly into the case of cyclic ratchetting by replacing Eq. (3) by Eq. (5) in the derivation of Eq. (7). The result we

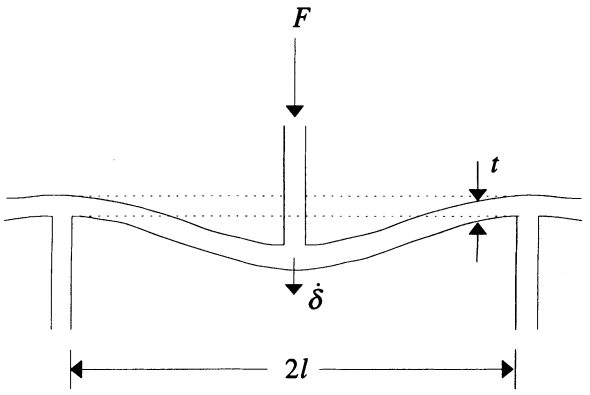

Fig. 9 Schematic of a cell edge loaded in bending. The cell edge ratchets, giving a deflection rate $\dot{\delta}$.

desire is

$$\frac{d\varepsilon}{dN} = C(1-R)^p \frac{0.6}{n+2}\left[\frac{1.7(2n+1)}{n}\frac{|\sigma|_{max}}{\sigma_0}\right]^n \bar{\rho}^{(3n+1)/2} \tag{8}$$

Equation (8) states the ratchetting rate for an open cell foam in terms of the ratchetting response [Eq. (5)] for the cell edge material, stress level and relative density of the foam. Although the Alulight foam investigated in the current study is a closed-cell foam, the cell faces are thin and defective compared to the cell edges, and the monotonic deformation and fracture response reflects that of an open-cell structure, as discussed in Refs [3,11].

The dependence of the fatigue limit upon stress level and relative density is estimated by assuming that the fatigue limit is attained when the accumulated plastic strain ε has attained a critical value ε_c equal to the monotonic yield strain ε_y of the foam. Integration of Eq. (8) then gives the fatigue life N_f as

$$\frac{1}{N_f} = \frac{C(1-R)^p}{\varepsilon_y}\frac{0.6}{n+2}\left[\frac{1.7(2n+1)}{\sigma_0}\frac{|\sigma|_{max}}{\sigma_0}\right]^n \bar{\rho}^{(3n+1)/2} \tag{9}$$

The experimental findings of the current study support the prediction

$$(|\sigma|_{max})^n N_f = \text{constant} \tag{10}$$

for both tension–tension and compression–compression fatigue. The data of the current study are insufficient to support or refute the predicted dependence of N_f upon relative density and load ratio, R.

OPEN-HOLE STRENGTH UNDER CYCLIC LOADING

Specimens containing a single central through-hole of diameter D were subjected to tension–tension and compression–compression fatigue loading in order to investigate the sensitivity of the cyclic strength to the presence of an open hole. The specimens, of length $L = 70$ mm, width $W = 20$ mm, thickness $B \sim 7.5$ mm and hole size $D/W = 0.1$–0.4 were made from the 0.6% Si foam of relative density $\bar{\rho} = 0.28$–0.36. The fatigue tests were performed along the longitudinal orientation, at several values of applied stress $|\sigma|_{max}/\sigma_y$, with $R = 0.1$.

The effect of hole diameter D on the tension–tension and compression–compression fatigue limits is summarized in Fig. 10, where we have written the fatigue limit as $|\sigma|_{max,n}$ for a notched specimen and $|\sigma|_{max,un}$ for an un-notched specimen. The fatigue strengths are compared with the net-section strength and the notch brittle predictions, defined as follows. The net-section strength criterion assumes that fatigue failure occurs when the net-section stress attains the fatigue limit for the un-notched material, giving

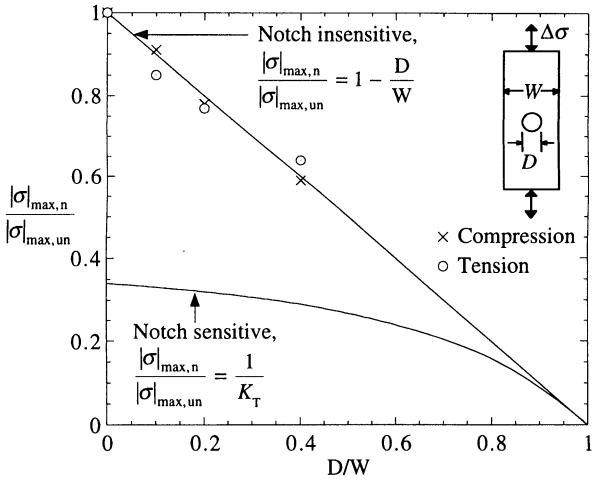

Fig. 10 Effect of an open hole on the endurance limit of Al–1Mg–0.6Si for compression–compression and tension–tension fatigue at $R = 0.1$. Specimens with $\bar{\rho} = 0.28$–0.36 which were tested in the longitudinal orientation.

$$\frac{\sigma_{max,n}}{\sigma_{max,un}} = 1 - \frac{D}{W} \tag{11}$$

The notch brittle criterion assumes that the material behaves in an elastic-brittle manner, such that fatigue failure occurs when the local stress at the edge of the hole attains the fatigue limit for the un-notched material. On writing the elastic stress concentration factor for the hole as K_T, the notch brittle criterion can be written as

$$\frac{\sigma_{max,n}}{\sigma_{max,un}} = \frac{1}{K_T} \tag{12}$$

The predictions given by Eqs (11) and (12) have been added to Fig. 10, by using Peterson's[16] calibration for K_T, which has the limit $K_T = 3$ for $D/W \ll 1$. It is concluded that Alulight behaves in a notch-insensitive manner under both tension–tension and compression–compression loading for the hole sizes considered: the fatigue limits follow the net-section strength criterion given by Eq. (11). Under compression–compression loading the foam behaves in a ductile manner, and this is the expected result. Under tension–tension loading the result is less obvious. It appears that the foam has sufficient ductility in the vicinity of the hole to diffuse the elastic stress concentration.

CONCLUSIONS

The tension–tension and compression–compression nominal stress versus fatigue life responses of Alulight closed-cell aluminium alloy foams have been measured

for the compositions Al–1Mg–0.6Si and Al–1Mg–10Si (wt%), and for relative densities in the range 0.1–0.4. Tests were performed at fixed load range, and the following main conclusions can be drawn.

1 The foam progressively lengthens under tension–tension loading, and progressively shortens under compression–compression loading, provided the load level exceeds a fatigue limit that has a value between 0.45 and 0.95 of the monotonic yield strength, depending on foam composition and density. The deformation mode comprises an initial stage of slow rate of strain accumulation. When the magnitude of the accumulated strain at maximum load of the fatigue cycle has attained a value of approximately the monotonic yield strain, the rate of strain accumulation increases by at least an order of magnitude. The knee of the accumulated strain versus cycles curve is used to define the fatigue life.
2 Under tension–tension loading, material separation occurs by the formation of a single dominant crack after the knee of the accumulated strain versus cycles curve. In contrast, under compression–compression loading, a crush band forms at the knee of the accumulated strain versus cycles curve, and large nominal strains (of the order of 50%) accumulate as the crush band intensifies and broadens.
3 The underlying mechanism of strain accumulation appears to be material ratchetting. Subsequent to the fatigue life, as defined in conclusion 1, cracking of the cell edges and faces ensues. A micromechanical model is given to predict the dependence of life upon stress level and relative density.
4 The fatigue strength of each foam increases with the relative density and mean applied stress, and is greater for the transverse orientation than for the longitudinal orientation. The foam of 10% Si content has a lower fatigue strength than the 0.6% Si foam, under compression–compression loading.
5 Tensile and compressive fatigue tests on specimens containing an open hole suggest that the fatigue limits of Alulight follow the net-section strength criterion: the foam behaves in a notch-insensitive manner for the three hole sizes considered.

Acknowledgements

The authors are grateful to the EPSRC and DARPA/ONR for their financial support, and to Dr F. Simancik of Mepura for supplying the Alulight foams.

REFERENCES

1 M. F. Ashby, A. G. Evans, N. A. Fleck, L. J. Gibson, J. W. Hutchinson and H. Wadley (in press) *Metal Foams: A Design Guide*. Butterworth-Heinemann.
2 J. Banhart and J. Baumeister (1998) Production methods for metallic foams. In: *Mat. Res. Soc. Symposium Proc.*, 521, p. 121.
3 K. Y. G. McCullough, N. A. Fleck and M. F. Ashby (1999) Uniaxial stress-strain behaviour of aluminium alloy foams. *Acta Mater.* **47**, 2323.
4 E. W. Andrews, G. Gioux, P. Onck and L. J. Gibson (in press) The role of specimen size, specimen shape and surface preparation in mechanical testing of metallic foams. *Int. J. Mech. Sci.*
5 Y. Sugimura, A. Rabiei, M. Y. He, A. G. Evans, A.-M. Harte and N. A. Fleck (1999) Compression fatigue of a cellular Al alloy. *Mater. Sci. Engng A.* **269**, 38.
6 Y. Sugimura, A. Rabiei, M. Y. He, H. Bart-Smith, J. Grenestedt and A. G. Evans (1997) On the mechanical performance of closed cell Al alloy foams. *Acta Mater.* **45**, 5245.
7 M. J. Silva and L. J. Gibson (1998) The effect of non-periodic microstructure and defects on the compressive strength of two-dimensional solids. *Int. J. Mech. Sci.* **39**, 549.
8 C. Chen, T. J. Lu and N. A. Fleck (1998) Effect of imperfections on the yielding of two-dimensional foams. *J. Mech. Phys. Solids* **47**, 2235.
9 A.-M. Harte, N. A. Fleck and M. F. Ashby (1999) Fatigue failure of an open cell and a closed cell aluminium alloy foam. *Acta Mater.* **47**, 2511.
10 O. B. Olurin, N. A. Fleck, M. F. Ashby (1999) Fatigue of aluminium alloy foam. In: *Proc. IFAM Metfoam 99 Conference on Metal Foams and Porous Metal Structures*, Bremen. MIT Publications, Bremen.
11 K. Y. G. McCullough, N. A. Fleck and M. F. Ashby (1999) Toughness of aluminium alloy foams. *Acta Mater.* **47**, 2331.
12 M. M. Megahed, A. R. S. Ponter and C. J. Morrison (1984) Experimental investigations into the influence of cyclic phenomena of metals on structural ratchetting behaviour. *Int. J. Mech. Sci.* **26**, 625.
13 L. J. Gibson and M. F. Ashby (1997) *Cellular Solids: Structures and Properties*, 2nd edition. Cambridge University Press, Cambridge.
14 C. E. Feltner and G. M. Sinclair (1963) Cyclic stress induced creep of close packed metals. In: *Joint Int. Conf. Creep, Inst. Mech. Engrs.*, Vol. 178, Part 3A, p. 7.
15 M. M. Megahed, A. R. S. Ponter and C. J. Morrison (1983) A theoretical and experimental investigation of material ratchetting in a beam element. *Int. J. Mech. Sci.* **25**, 917.
16 R. E. Peterson (1974) *Stress Concentration Design Factors*. John Wiley, London.